

for the  $F$  center. 3. The different temperature dependences of the emission of the two  $F_H$ -band components has to be compared with the results of Lynch, Brothers, and Robinson<sup>3</sup> for the  $F$  center. However, although these authors do not reveal this property, their excitation spectrum shows more structure than the absorption spectrum. Both were only measured at 13°K. It would be interesting to measure the low-temperature behavior of the emission for the two components of the  $F$  band using a narrow spectral bandwidth for excitation.

In the case of the  $F_H$  center, the excited state is still split up after lattice relaxation. The temperature behavior of the emission of the 590-nm component at low

<sup>3</sup> D. W. Lynch, A. D. Brothers, and D. A. Robinson, *Phys. Rev.* **139**, A285 (1965).

temperatures seems to indicate that it is thermally activated. The appearance of only one structureless emission band could indicate that the luminescence starts from one single level. Measurements of the radiative lifetime at low temperatures for the two components could perhaps give more information about the luminescence mechanism.

#### ACKNOWLEDGMENTS

We wish to thank Professor W. Dekeyser for his continuous interest during this investigation. This work is part of a research program sponsored by "l'Institut pour l'Encouragement de la Recherche Scientifique dans l'Industrie et l'Agriculture."

### Optical Phonons in Sodium Chlorate

C. M. HARTWIG, D. L. ROUSSEAU,\* AND S. P. S. PORTO

*Department of Physics and Electrical Engineering, University of Southern California,  
Los Angeles, California 90007*

(Received 17 July 1969)

The frequencies of the optical phonons in NaClO<sub>3</sub> have been located by measuring the infrared reflectivity and the Raman scattering spectra. By using the Lyddane-Sachs-Teller relationship, a value of 5.6 was found for the static dielectric constant. Dielectric transition strengths were determined from the transverse-longitudinal frequency splitting and found to agree well with prior values obtained by analyses of infrared data. The reflection spectrum, the index of refraction, and the absorption coefficient have been determined throughout the range of the lattice resonances.

#### INTRODUCTION

WITHIN the past few years, since the application of the laser to the technology of Raman spectroscopy, scattering from several crystals has been studied. In general, the emphasis has been placed on single uniaxial ionic crystals where the complexity of the spectrum was compatible with the development of the theoretical understanding. Considerable emphasis is now being devoted to the more complex crystals, including those of low symmetry with few atoms per unit cell and those of high symmetry with many atoms per unit cell. Sodium chlorate is an excellent representative example of the latter case. It is cubic, belonging to the  $T^4$  space group,<sup>1</sup> and is, therefore, also optically active. There are 4 molecules (20 atoms) per unit cell, resulting in 60 degrees of freedom. The lattice is ionic, consisting of sodium and chlorate ions. Furthermore, the chlorate ions show strong intraionic forces and may therefore be treated as a unit, giving the material molecular-crystal-like features.

Several Raman studies of NaClO<sub>3</sub> have been made in the past.<sup>2-5</sup> However, the results of these early investigations were not reliable, since there were "extra" lines in some regions of the spectrum and "missing" lines in other regions. In addition, different frequency values were obtained by each investigator, and there was disagreement as to the assignments of observed lines. These inconsistencies may have resulted from any of several effects. First, NaClO<sub>3</sub> is optically active.<sup>6</sup> When laser sources were not available, it was necessary to illuminate a large volume of the crystal to obtain sufficient intensity to make Raman observations. Large crystalline dimensions allowed appreciable angles of optical rotation, and subsequent depolarization errors in the spectra then resulted. Secondly, the point group of sodium chlorate ( $T$ ) contains  $A$  and  $E$  irreducible representations, both of which have only diagonal com-

<sup>2</sup> A. Rousset, J. Laval, and R. Lochet, *Compt. Rend.* **216**, 886 (1943).

<sup>3</sup> L. Couture and J. P. Mathieu, *Ann. Phys. (Paris)* **12**, 521 (1948).

<sup>4</sup> V. Chandrasekharan, *Proc. Indian Acad. Sci.* **32A**, 374 (1950).

<sup>5</sup> H. Poulet, *Ann. Phys. (Paris)* **10**, 908 (1955).

<sup>6</sup> *International Critical Tables* (McGraw-Hill Book Co., New York, 1930), Vol. III, p. 353.

\* Present address: Bell Laboratories Inc., Murray Hill, N. J.

<sup>1</sup> R. W. G. Wykoff, *Crystal Structures* (Wiley-Interscience, Inc., New York, 1957), Vol. II, Chap. VII, p. 5.

ponents. This makes phonons of these symmetries very difficult to distinguish from each other, unless very careful experimental arrangements are used. Thirdly, there are several phonons in the crystal which are simultaneously infrared and Raman active. When such a mode is observed in the Raman effect, the long-range electric field associated with the vibration splits the phonon into a transverse and a longitudinal component of different frequencies, thereby further complicating an already rich Raman spectrum.

The infrared absorption and reflectivity spectrum have been obtained previously in the region of the internal chlorate ion lattice vibrations,<sup>7-9</sup> but not in the region of the external librational and translational modes. In the most recent study by Andermann and Dows,<sup>8,9</sup> the authors concluded that the proximity of some longitudinal frequencies to each other invalidated the Lyddane-Sachs-Teller (LST) relationship in this crystal. Also when they calculated dielectric transition strengths, there were large discrepancies among values obtained by different methods.

In order to clarify these several ambiguities and discrepancies, we have obtained the complete Raman spectrum of sodium chlorate. The low-frequency (40–400  $\text{cm}^{-1}$ ) infrared reflectivity spectrum was also determined. In addition, by carefully measuring the Raman spectrum under several different orientations, the dependence of the frequency on the phonon propagation direction has been studied. From an analysis of our data, dielectric transition strengths, damping constants, and the static permittivity have been calculated.

### THEORY

$\text{NaClO}_3$  belongs to the space group  $T^4$  ( $P2_13$ ) and has 4 molecular units per primitive cell.<sup>1</sup> It is convenient to separate the vibrational problem into two separate regions—the chlorate ion internal mode frequency region ( $\sim 400$ – $1100$   $\text{cm}^{-1}$ ) and the librational and translational external mode region ( $\sim 40$ – $400$   $\text{cm}^{-1}$ ). From group theory the degrees of freedom of the  $C_{3v}$  chlorate ion may be divided into  $3A_1 + 1A_2 + 4E$  irreducible representations.<sup>10</sup> The three modes belonging to the  $A_1$  representation consist of  $\nu_1$  and  $\nu_2$  internal vibrations as defined by Herzberg<sup>11</sup> and a translation in the  $z$  direction; the vibration of  $A_2$  symmetry is a rotation about  $z$ ; and the four modes of  $E$  symmetry are  $\nu_3$  and  $\nu_4$  internal vibrations, a degenerate translation, and a degenerate rotation. Both the chlorate and the sodium

<sup>7</sup> J. L. Hollenberg and D. A. Dows, *Spectrochim. Acta* **16**, 1155 (1960).

<sup>8</sup> G. Andermann and D. A. Dows, *J. Phys. Chem. Solids* **28**, 1307 (1967).

<sup>9</sup> G. Andermann, Ph.D. dissertation, University of Southern California, 1965 (unpublished).

<sup>10</sup> D. L. Rousseau, R. P. Bauman, and S. P. S. Porto (unpublished).

<sup>11</sup> G. Herzberg, *Molecular Spectra and Molecular Structure: II. Infrared and Raman Spectra of Polyatomic Molecules* (D. Van Nostrand, Inc., Princeton, N. J., 1945), p. 110.

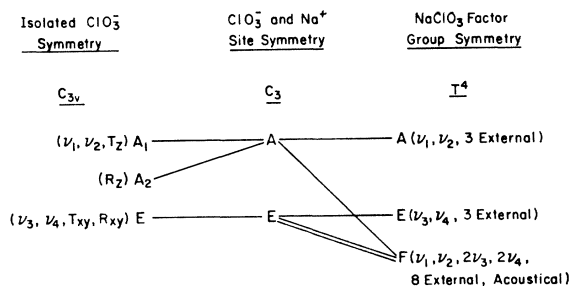


FIG. 1. Correlation table for  $\text{NaClO}_3$ .

ions occupy  $C_3$  sites in the cubic lattice. The correlation diagram in Fig. 1 maps out the site splitting and the factor-group splitting (correlation-field splitting), which might be expected in crystalline  $\text{NaClO}_3$ . On the basis of this analysis the degrees of freedom of all the atoms in the primitive cell should be split into  $5A + 5E + 15F$  symmetry modes. The acoustic phonon belongs to the  $F$  representation, leaving fourteen  $F$  optical branches. On the basis of the factor-group splitting, the crystal spectrum should show phonons of  $A$  and  $F$  symmetry in the region of the  $\nu_1$  mode of the free ion (930  $\text{cm}^{-1}$ ).<sup>12</sup> Similarly, in the region of  $\nu_2$  (610  $\text{cm}^{-1}$ ) there should be  $A$  and  $F$  symmetry phonons.  $\nu_4$  (497  $\text{cm}^{-1}$ ) and  $\nu_3$  (982  $\text{cm}^{-1}$ ) should each split into an  $E$  mode and two  $F$  modes. In the region of external modes there should be  $3A + 3E + 8F$  optical branches.

The  $A$ ,  $E$ , and  $F$  symmetry phonons are all Raman active. The phonons belonging to the  $F$  representation are also infrared active causing longitudinal-transverse frequency splitting. The Raman tensors associated with each of these species are presented below:

$$A = \begin{pmatrix} a & 0 & 0 \\ 0 & a & 0 \\ 0 & 0 & a \end{pmatrix},$$

$$E = \begin{pmatrix} b & 0 & 0 \\ 0 & b & 0 \\ 0 & 0 & -2b \end{pmatrix} \begin{pmatrix} \sqrt{3}b & 0 & 0 \\ 0 & -\sqrt{3}b & 0 \\ 0 & 0 & 0 \end{pmatrix},$$

$$F(x) = \begin{pmatrix} 0 & 0 & 0 \\ 0 & 0 & c \\ 0 & c & 0 \end{pmatrix},$$

$$F(y) = \begin{pmatrix} 0 & 0 & c \\ 0 & 0 & 0 \\ c & 0 & 0 \end{pmatrix},$$

$$F(z) = \begin{pmatrix} 0 & c & 0 \\ c & 0 & 0 \\ 0 & 0 & 0 \end{pmatrix}.$$

Modes of  $A$  and  $E$  symmetry are inactive in the infrared and consequently have no polarization associated with them. The polarization associated with the  $F$  symmetry phonons is indicated in parentheses.

<sup>12</sup> S. T. Shen, Y. T. Yao, and Ta-You Wu, *Phys. Rev.* **51**, 235 (1937).

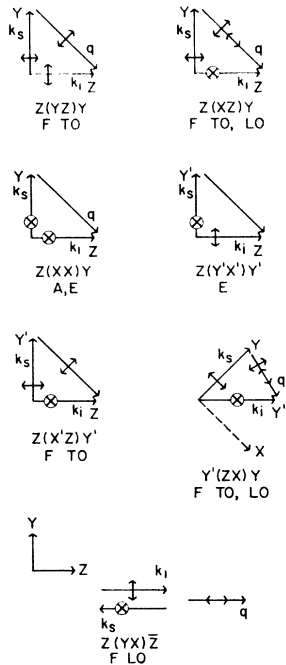


FIG. 2. Scattering diagrams for all arrangements discussed in this paper. The incident beam direction is  $k_i$  and the scattered direction is  $k_s$ . The corresponding phonon propagation direction is indicated by  $q$ . The polarization vectors are indicated by the shorter arrows. Primed coordinates are those resulting from a 45° rotation of the crystal about the  $z$  axis.

Since all fourteen  $F$  modes carry charge, they may interact with infrared radiation through the absorption and the reflection of light. The reflectivity  $R$  is given by

$$R(\omega) = \left| \frac{[\sqrt{\epsilon(\omega)}] - 1}{[\sqrt{\epsilon(\omega)}] + 1} \right|^2, \quad (1)$$

where  $\epsilon(\omega)$  is the frequency-dependent dielectric constant, which is related to the index of refraction,  $n$ , and the extinction coefficient  $\kappa$  by

$$\epsilon(\omega) = (n - i\kappa)^2. \quad (2)$$

Moreover, the relative permittivity is related to a system's resonances  $\omega_{0j}$ , the dielectric transition strengths  $S_j$ , the damping constants  $\gamma_j$ , and the high-frequency dielectric constant  $\epsilon_\infty$ , by the expression

$$\epsilon(\omega) = \epsilon_\infty + \sum_j \frac{S_j \omega_{0j}^2}{\omega_{0j}^2 - \omega^2 + i\gamma_j \omega}. \quad (3)$$

At transverse phonon frequencies  $\omega_{TO}^j$ , the complex permittivity is infinite and at longitudinal phonon frequencies,  $\omega_{LO}^j$ , it is zero. In reflectivity experiments, both the TO and the LO values may be determined from inflection points in the spectrum.<sup>13</sup> In the Raman

<sup>13</sup> C. Haas and D. F. Hornig, *J. Chem. Phys.* **26**, 707 (1957); E. Burstein, in *Dynamical Processes in Solid State Optics*, edited by

scattering spectrum these phonons appear as separate lines.

The generalized LST relationship, first derived by Cochran and Cowley,<sup>14</sup> may be expressed by the following:

$$\frac{\epsilon_0}{\epsilon_\infty} = \prod_i \left( \frac{\omega_{LO}^i}{\omega_{TO}^i} \right)^2, \quad (4)$$

in which  $\epsilon_0$  is the static dielectric constant, and the product is taken over all the polar phonon frequencies. In the derivation of this generalized relationship, an approximation was made in which the crystal was assumed to be composed of a system of harmonic oscillators without damping. This should be the only possible source of deviation from the LST in a  $\text{NaClO}_3$  crystal. Furthermore, Cochran and Cowley<sup>14</sup> have estimated that the maximum deviation from Eq. (4) from anharmonic effects that might be expected for real crystals is about 5%.

## EXPERIMENTAL

A large solution-grown single crystal of  $\text{NaClO}_3$  was provided to us by Dows, of the Chemistry Department of the University of Southern California. From this, smaller crystals were then cut with faces in (100) and (110) planes, and the orientation was confirmed by x-ray diffraction. Final polishing of each crystal was performed with a slurry of Linde B in ethyl alcohol upon a Pellon R pad.

In the Raman experiments, the spectra were obtained with a laser which was built in our laboratory and had a dc-excited argon plasma. Two of the argon ion laser lines at 5145 and 4880 Å were used. By using the second line, ghosts, fluorescence, and other wavelength-dependent phenomena could be readily discerned. The spectrometer was the Spex Double Monochromator-Model 1400-11. In general, data were obtained at room temperature, but one set of experiments was done at 20°K. The crystal was cooled by placing it in a Dewar and blowing a boil-off from liquid helium over it. Frequencies were measured to an absolute accuracy of about  $\pm 1 \text{ cm}^{-1}$ . The electronic limit of our detectability is about 10 photoelectron pulses per second in the present experiments. This corresponds to total emission of about  $10^4$  photons/sec from our sample.

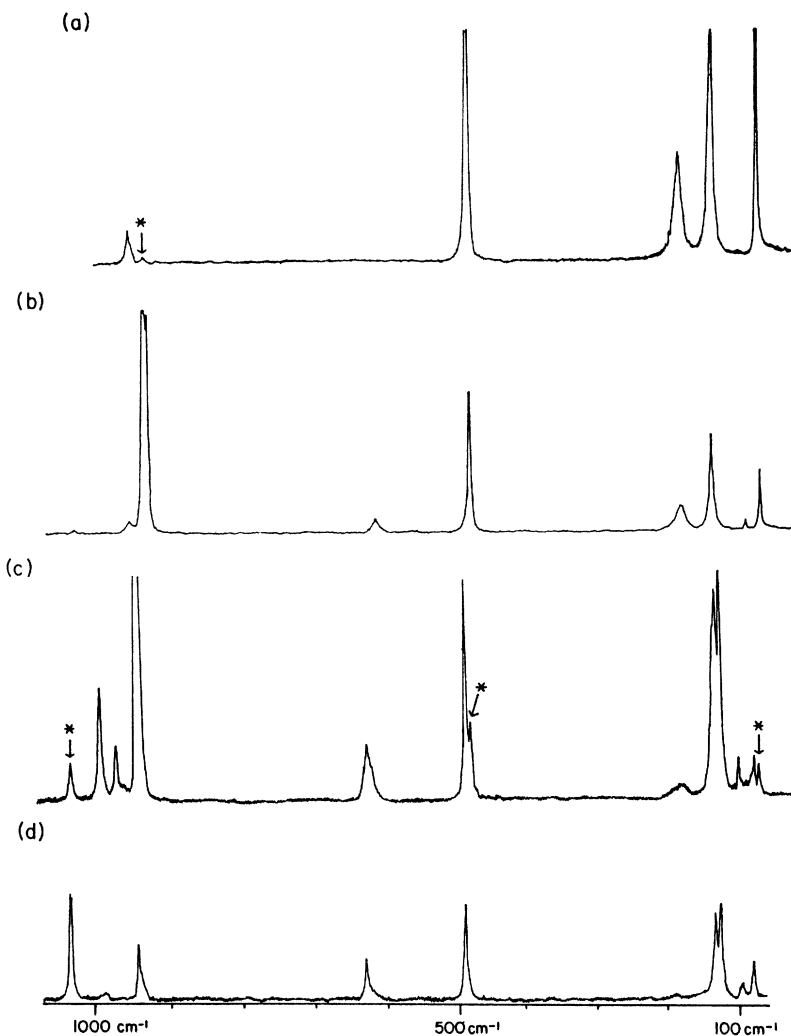
In the Raman experiments, the geometrical arrangement of the incident and scattered light polarizations and of the incident and scattered propagation directions were carefully selected to study each of the Raman tensor components. The standard notations<sup>15</sup> of the type  $k(ij)q$  are used throughout this paper to indicate the

R. Kubo and H. Kamimura (W. A. Benjamin, Inc., New York, 1967), pp. 1-33.

<sup>14</sup> W. Cochran and R. A. Cowley, *J. Phys. Chem. Solids* **23**, 447 (1962).

<sup>15</sup> T. C. Damen, S. P. S. Porto, and B. Tell, *Phys. Rev.* **142**, 570 (1966).

FIG. 3. Survey Raman spectra of  $\text{NaClO}_3$ . The \* indicate lines that occur in the spectrum as a result of spillover from other symmetries because of slight misorientation and depolarization effects. (a)  $z(y'x')y'$  spectrum showing  $E$  phonons. (b)  $z(xx)y$  spectrum in which both  $A$  and  $E$  phonons are present. (c)  $z(x'z)y'$  spectrum of the  $F$  TO modes. (d)  $z(yx)z$  spectrum displaying the  $F$  LO phonons.



scattering geometry, where  $k$  is the propagation direction of the incident light,  $i$  is the polarization direction of incident light,  $j$  is the polarization direction of scattered light, and  $q$  is the propagation direction of scattered light.

For  $A$  and  $E$  phonons, which are not polar, a unique single frequency is obtained for each mode. However, for the polar  $F$  modes, it is necessary to simultaneously consider the polarization direction and the propagation direction<sup>16,17</sup> (via the conservation of wave vector) to predict the occurrence of transverse or longitudinal phonons. This prediction can be most easily made through the use of scattering diagrams which are shown in Fig. 2 for all geometries discussed in this paper.

In the representation of the Raman tensor, using the crystallographic axes as the basis set, both  $A$  and  $E$  species have only diagonal components. It is possible to

separate the  $E$  species from the  $A$  species by orienting polarizations at  $45^\circ$  angles with respect to the crystallographic axes. By performing this rotation the  $A$  tensor is unchanged, but the  $E$  tensor acquires off-diagonal components. The various rotated orientations are indicated by primed coordinates. All appropriate scattering diagrams are included in Fig. 2.

The  $4.1^\circ/\text{mm}$  (at  $5200 \text{ \AA}$ ) optical activity<sup>6</sup> of  $\text{NaClO}_3$  presents a problem which, if not recognized, could cause apparent selection rule breakdowns. This problem was minimized with proper experimental techniques. When a right-angle scattering experiment was performed, light entered the crystal within 2 mm of the crystal face closest to the spectrometer. Furthermore, only the first 2 mm of the laser light's threadlike passage through the crystal was focused on the spectrometer slit. For back scattering a cleaved crystal of 2 mm thickness was used.

Reflection measurements from 40 to  $400 \text{ cm}^{-1}$  were made with a Perkin-Elmer—Model 301, far-infrared double-beam spectro-photometer. The dove-tailed back

<sup>16</sup> R. Loudon, *Advan. Phys.* **13**, 423 (1964).

<sup>17</sup> C. A. Arguello, D. L. Rousseau, and S. P. S. Porto, *Phys. Rev.* (to be published).

TABLE I. Optical phonons of NaClO<sub>3</sub>. All values are expressed in cm<sup>-1</sup>. The damping constants are those measured for the TO phonons.

<i>A</i>	<i>E</i>	Raman		Infrared		Damping constant <i>γ</i>	
		<i>F</i> (TO)	<i>F</i> (LO)	<i>F</i> (TO)	<i>F</i> (LO)		
65	86	72	78	72	78	5	
		95	97			4	
		124	125			4	
134	134	131	133	142	154	7	
						12	
						20	
	180	183	183	176	190	30	
					202	220	15
					481.5 <sup>a</sup> ( <i>ν</i> <sub>4</sub> )	485.2 <sup>a</sup>	4
	482( <i>ν</i> <sub>4</sub> )	489( <i>ν</i> <sub>4</sub> )	490	624.0 <sup>a</sup> ( <i>ν</i> <sub>2</sub> )		4	
618( <i>ν</i> <sub>2</sub> )		623( <i>ν</i> <sub>2</sub> )	629			5	
932 <sup>b</sup>		931 <sup>b</sup>	932 <sup>b</sup>			4	
937( <i>ν</i> <sub>1</sub> )	957( <i>ν</i> <sub>3b</sub> )	936( <i>ν</i> <sub>1</sub> )	940	937.5 <sup>a</sup> ( <i>ν</i> <sub>1</sub> )		4	
		965( <i>ν</i> <sub>3b</sub> )	983	966.4 <sup>a</sup> ( <i>ν</i> <sub>3b</sub> )		5	
		988( <i>ν</i> <sub>3a</sub> )	1030	987.2 <sup>a</sup> ( <i>ν</i> <sub>3a</sub> )		1027 <sup>a</sup>	5

<sup>a</sup> Values determined in Ref. 8.  
<sup>b</sup> *ν*<sub>1</sub> isotope frequencies.

surfaces of the room-temperature crystal had rough and irregular faces, consequently minimizing back-surface scattering. An unpolarized beam struck the crystal's face at 9° with respect to the surface normal. In making calculations of reflectivity a correction was made for this small perturbation from the standard analysis of perpendicular and polarized radiation striking a dielectric.

## RESULTS

Figure 3 shows the Raman spectra of NaClO<sub>3</sub> obtained at 25°C for several scattering geometries. The data from these experiments are summarized in Table I along with our assignments. The identification of all the *F*-symmetry LO and TO phonons is unambiguous except for the mode at 183 cm<sup>-1</sup>. This line is broad, weak, and asymmetrical, making an accurate assignment tenuous. We believe, however, it is a distinct *F* phonon mode. It has an interesting temperature dependence,<sup>18</sup> which is presently being studied. In the external-mode region of the spectrum only five Raman frequencies of *F* symmetry were found. Group theory predicts the existence of eight such frequencies. Resolution as good as 1 cm<sup>-1</sup> did not reveal the presence of the three missing lines. A low-temperature experiment (*T* = 20°K), having sharpened the Raman lines to a width of 3 cm<sup>-1</sup>, still showed no additional lines. A comparison of a calculation of the static dielectric constant from the generalized LST expression using 11 LO-TO Raman phonons (external and internal), to a known value of the low-frequency dielectric constant revealed a huge discrepancy. Our calculated dielectric constant was much lower than the measured one. This directed us toward an infrared reflection experiment to look for the missing modes. The

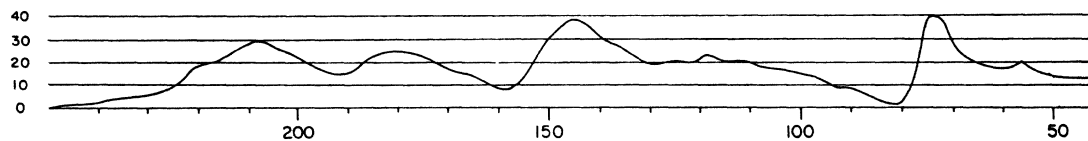
results of this experiment are shown in Fig. 4 and summarized in Table I, where the LO-TO frequency sets and damping constants found in the infrared experiment are also tabulated. These values were obtained from the reflection spectra in the following way. Transition strengths *S<sub>j</sub>* were calculated from the *k* equations

$$\epsilon(\omega_{\text{LO}}^k) = \epsilon_\infty + \sum_{j=1}^N \frac{(\omega_{\text{TO}}^j)^2 S_j}{(\omega_{\text{TO}}^j)^2 - (\omega_{\text{LO}}^k)^2} = 0, \quad (5)$$

in which the sum is over all the polar phonons. From these values a reflectivity curve was calculated, using Eqs. (1) and (3), and compared to the measured spectrum. The initial estimates of  $\omega_{\text{TO}}^j$ ,  $\omega_{\text{LO}}^j$ , and  $\gamma_j$  (obtained from the reflection data) were then modified to obtain a new set of *S<sub>j</sub>*'s and a better fit to the reflectivity spectrum. This process was repeated until the best fit between the computed curve and the empirical spectrum was obtained. All eight external modes are then accounted for from the combination of both experiments. The absence of four of the vibrations in our reflection data is explained by these lines's low dielectric transition strength, as exhibited by their weak LO-TO splitting in the Raman data.

In the internal-mode region there should be an *F* symmetry phonon in the region of each *ν*<sub>1</sub> and *ν*<sub>2</sub>, and two *F* phonons near each *ν*<sub>3</sub> and *ν*<sub>4</sub>. In our Raman spectra five of these six LO-TO pairs were found, since only one *F* symmetry LO-TO pair could be detected in the *ν*<sub>4</sub> region. The infrared data,<sup>8</sup> however, also showed only one transverse-longitudinal pair in the *ν*<sub>4</sub> region with different frequencies than our Raman values. Hence from these two experiments both *F* modes can be accounted for. One of those modes is strongly Raman active and weakly infrared active, and the other displays the opposite intensity relationship. There are a total of four modes of *F* symmetry that are too weakly Raman active to be observed in our experiments. The

<sup>18</sup> V. S. Gorelik, I. V. Gavrilova, I. S. Zheludev, G. V. Peregudov, V. S. Ryazanov, and M. M. Sushchinskii, Zh. Eksperim. i Teor. Fiz. Pis'ma v Redaktsiyu 5, 169 (1967) [English transl.: Soviet Physics—JETP Letters 5, 171 (1967)].

FIG. 4. Low-frequency infrared reflection spectrum of  $\text{NaClO}_3$ .

critical factor that makes symmetry-allowed Raman lines very weak is the matrix elements for the electron-lattice coupling. A weak Raman line indicates a weak electron-phonon interaction. We are currently examining the effect of crystal symmetry upon the lattice modes and consequently upon the electron-lattice matrix elements.

The  $A+E$  spectra are shown in Fig. 3(b) and pure  $E$  phonons in Fig. 3(a). Among the  $A$  symmetry modes the line at  $134\text{ cm}^{-1}$  is coincident with an  $E$  line. An intensity decrease of the  $134\text{ cm}^{-1}$  line in the  $E$  spectra as compared to  $A$  and  $E$  combination spectra revealed the existence of the  $A$  mode. The  $A$  symmetry line at  $65\text{ cm}^{-1}$  was used as a reference in the two experiments. There is a missing line in the  $A$  symmetry Raman spectra. The missing vibration is an external mode. This  $A$  mode is again either too weak to observe or is obscured by an accidental degeneracy, and since it is infrared inactive it cannot be observed in the infrared spectrum.

Chlorine appears naturally as  $^{37}\text{Cl}$  and  $^{35}\text{Cl}$ .  $^{37}\text{Cl}$  exists in about  $\frac{1}{3}$  the abundance of  $^{35}\text{Cl}$ . Hollenberg and Dows<sup>7</sup> have calculated expected isotope shifts of the eigenfrequencies of the internal vibrations. In our experiments only one internal vibration ( $\nu_1$ ) exhibited resolvable isotope dependence.

The frequencies of the longitudinal and transverse phonons were determined, respectively, from experiments in which the propagation direction was  $\mathbf{k} = k\hat{z}$ ,  $[z(yx)\hat{z}]$ , and  $\mathbf{k} = k(\frac{1}{2})^{1/2}(\hat{y} + \hat{z})$ ,  $[z(yz)y]$  (refer to Fig. 2). An additional TO spectrum was excited

with the odd propagation direction of  $\mathbf{k} = k[\frac{1}{2}(\hat{x} - \hat{y}) + (\frac{1}{2})^{1/2}\hat{z}]$ ,  $[z(x'z)\hat{y}']$ . The TO eigenvalues from both experiments agreed within an experimental error of  $0.6\text{ cm}^{-1}$ .

To determine the effect of off-axis propagation directions, coupled with a predicted mechanical polarization that is neither transverse nor longitudinal, two additional spectra were obtained—one in which the phonon was forced to propagate in the direction  $\mathbf{k} = k(\frac{1}{2})^{1/2}(\hat{y} + \hat{z})$ ,  $[z(xz)\hat{y}]$ , and one in which the propagation direction was  $\mathbf{k} = k[\hat{x} + (\sqrt{2} - 1)\hat{y}][4 - 2\sqrt{2}]^{-1/2}$ ,  $[y'(zx)y]$ . The results of these experiments are presented in Table II. The resolvable eigenvalues are now the same as the previously measured LO and TO frequencies. A phonon with a mechanical polarization, induced at an acute angle to its direction of travel, is resolved into an LO and a TO component. For a few combinations of LO and TO frequencies the two lines appear as one, because their small splitting and large linewidth yield a single-valued resultant intensity. Also when the polarization direction has a large component in the phonon propagation direction, the LO may become the dominantly excited line, thereby obscuring the weak TO phonon.

## DISCUSSION

Rosenstock<sup>19</sup> has concluded on the basis of a two-dimensional model that in cubic crystals if phonons propagate in directions other than along the main

TABLE II. Raman values ( $\text{cm}^{-1}$ ) of polar phonons for off-axis propagation and polarization directions.

$Z(XZ)Y$	$Y'(ZX)Y$
72 TO	72 TO
77 LO	78 LO
96 <sup>a</sup>	96 <sup>a</sup>
124 <sup>a</sup>	125 <sup>a</sup>
131 TO	134 LO
184 <sup>a</sup>	
490 LO	490 LO
622 TO	
629 LO	629 LO
931 TO	932 LO
936 TO	936 TO
940 LO	940 LO
965 TO	
983 LO	983 LO
987 TO	
1030 LO	1030 LO

<sup>a</sup> TO and LO could not be separately resolved.

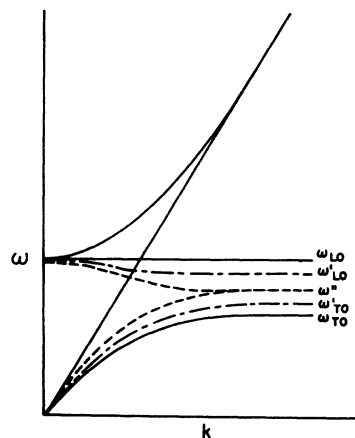


FIG. 5. Hypothetical dispersion curves exemplifying the various possibilities of what might occur if the pure transverse or pure longitudinal character is not preserved in off-axis propagation directions.

<sup>19</sup> H. R. Rosenstock, Phys. Rev. **121**, 416 (1961).

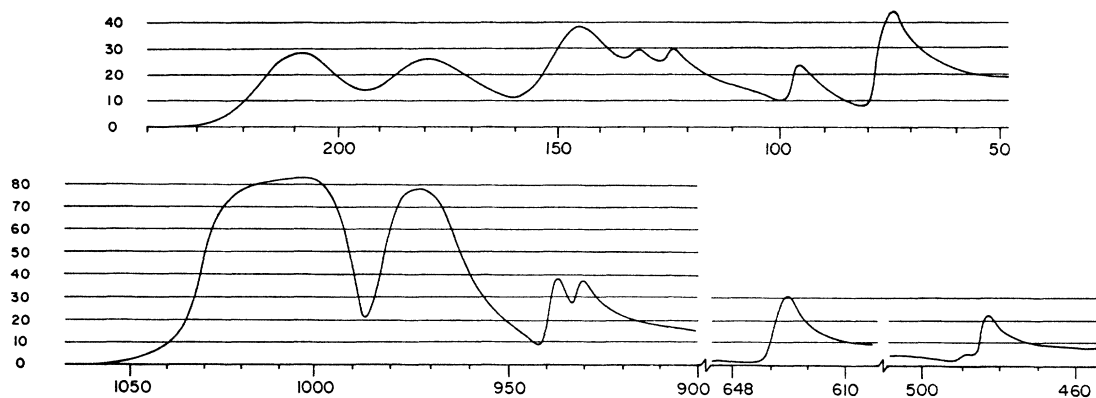


FIG. 6. Calculated infrared reflectivity spectrum.

crystallographic directions they no longer remain strictly transverse or longitudinal. Raman scattering provides a very sensitive probe of the transverse or longitudinal character of phonons, since the propagation direction may be readily selected, and the frequencies of the phonons may be monitored. The spectra of a phonon propagating in a general direction should then show a breakdown of the longitudinal-transverse character.

$\text{NaClO}_3$  has many types of polar phonons. Some are external; some are internal; some have large LO-TO frequency splitting; and some have small LO-TO splitting. The crystal, therefore, provides for a complete test of Rosenstock's theory. If any deviation from pure longitudinal or pure transverse modes were to exist in a cubic crystal, a frequency shift, as exemplified in the dispersion curve of Fig. 5, should occur in the  $\text{NaClO}_3$  spectrum. If this longitudinal-transverse character breakdown is small, it would result in only a small-frequency shift from the resonant LO and TO frequencies, corresponding to  $\omega_{\text{LO}}'$  and  $\omega_{\text{TO}}'$  of Fig. 5. On the other hand, if the LO-TO mixing is very large, the longitudinal and transverse distinction would be removed. If such a situation occurred in  $\text{NaClO}_3$ , the  $y'(zx)y$  and  $z(xz)y$  experiments would display only a

single frequency for each LO-TO pair, and this frequency would be somewhere intermediate between the "pure" LO and TO values. This is indicated by  $\omega''$  in Fig. 5. The failure to observe any frequency shifting as a function of propagation angle for all the polar phonons implies that for small- $k$  optical phonons in cubic crystals the electrostatic character is conserved independent of propagation direction. In this regard the LST relationship will not be invalidated, since the phonons will always retain the resonant values. This experimental conclusion is in contrast to Rosenstock's theoretical deductions.

The LST relationship holds in all crystals that do not exhibit severe anharmonicities, and it should therefore hold in  $\text{NaClO}_3$  in spite of near accidental degeneracy of several pairs of phonons. In our determination of the static permittivity by the LST relation care was taken to include all 15 polar phonons by selecting the very accurate Raman frequencies whenever possible (five internal modes, five external modes, and one isotope mode) and using the reflectivity data for the remaining modes [three external and one ( $\nu_4$ ) internal]. The value of  $\epsilon_0$  obtained from Eq. (4) was 5.6. This agrees well

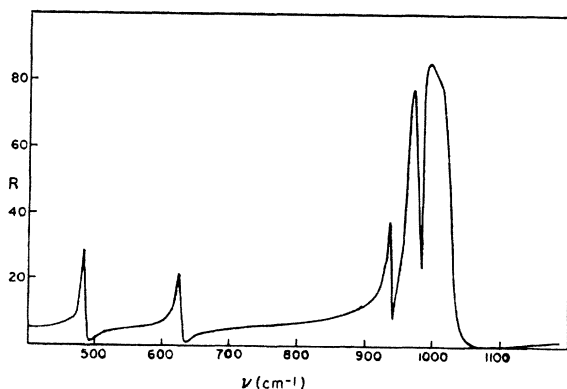


FIG. 7. Infrared reflectivity spectrum of the internal-mode region taken from Ref. 8.

TABLE III. Transition strengths  $S_j$  determined from Eq. (5). For comparison, values obtained in Ref. 8 are included.

$F(\text{TO})$	$S_j$	$S_j \omega_j^2 \text{ (cm}^{-2}\text{)}$	$S_I \text{ (cm}^{-2}\text{) from Ref. 8}$
72	0.997	5170	
95	0.197	1780	
124	0.147	2200	
131	0.254	4310	
142	0.686	13 800	
176	0.483	15 000	
183	0.0		
202	0.188	7690	
482	0.037	8600	11 800
489	0.006	1500	
623	0.051	20 000	16 700
931	0.023	20 200	
936	0.038	33 000	48 200
965	0.195	182 000	164 200
988	0.037	37 000	41 800

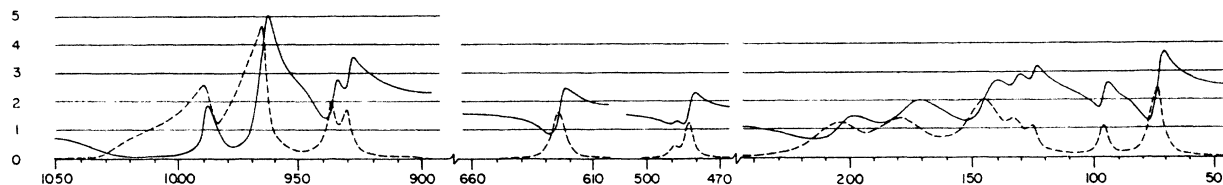


FIG. 8. Calculated curves of the refractive index (solid line) and the extinction coefficient (dashed line).

with a value of 5.7 measured at 10 kc by Mason.<sup>20</sup> The effects of anharmonicity have been considered explicitly by Barker.<sup>21</sup> However, in the case of  $\text{NaClO}_3$ , in which the linewidth of all the polar phonons is small compared to the phonon frequency, the correction may be neglected, and the usual form of the generalized LST may be used.

Andermann and Dows,<sup>8</sup> in studying the reflectivity spectrum of the internal modes of sodium chlorate, determined transition strengths ( $S$ ) by four methods. They stated that the most reliable technique, in terms of reproducing the experimental spectrum, was one in which the dielectric transition strengths were determined by integrating over the product of the absorption coefficient and the index of refraction. Values of  $S$  were also determined by Andermann and Dows by using expressions of the type

$$S_j \propto [(\omega_{LO}^j)^2 - (\omega_{TO}^j)^2]. \quad (6)$$

In their study there was a striking lack of agreement between the transition strengths determined by these techniques. Their other two methods are of little value and will not be discussed here.

Equation (6) may be derived by selecting only a single set of values in the summation of Eq. (3) (neglecting damping) and, as expected, enjoyed moderate success, when the resonance involved is distant from other resonances. However, in  $\text{NaClO}_3$  where there are several resonances located close to one another, it becomes necessary to evaluate the various  $S_j$ 's simultaneously, since the effect of neighboring phonons is appreciable. The failure to do this in Ref. 8 resulted in the large differences in transition strengths as determined by these two techniques. The transition strengths

in the present study came from Eq. (5). These are given in Table III. The results of this analysis agree very well with the experimental oscillator strengths determined by Andermann and Dows,<sup>8</sup> also listed in Table III, by the integration over the absorption coefficient and the refractive index, and establish, contrary to a conclusion reached in Ref. 8, that the polar phonon frequency analysis is a useful and accurate method for determining transition strengths.

A further confirmation of the validity of Eq. (3) may be obtained by using it to calculate a complete reflectivity spectrum through the relationship presented in Eq. (1). Figure 6 is a complete plot of a calculated reflectivity spectrum in the infrared region determined solely from phonon frequencies and linewidths. For comparison the measured internal-mode region reflectivity spectrum<sup>8</sup> is given in Fig. 7. The frequency values used in constructing the calculated spectrum were only accurate to  $\pm 1 \text{ cm}^{-1}$  resulting in some variation in the comparison with the experimental spectrum. The index of refraction,  $n$ , is the real part of the square root of the dielectric constant and the extinction coefficient  $\kappa$  is the imaginary part of it. These two functions are plotted as a function of frequency in Fig. 8. The agreement between the reflectivity calculated from the Raman frequencies and the measured reflectivity of the internal-mode infrared analysis demonstrates the great utility of Raman spectroscopy in the determination of such fundamental physical properties of crystals.

#### ACKNOWLEDGMENTS

We wish to thank Dr. C. A. Arguello and Dr. R. Luzzi for several helpful discussions and W. G. Spitzer for his valuable assistance with our experiments. Support from the National Science Foundation is gratefully acknowledged.

<sup>20</sup> W. P. Mason, Phys. Rev. **70**, 529 (1946).

<sup>21</sup> A. S. Barker, Jr., Phys. Rev. **136**, A1290 (1964).